Contrib Mineral Petrol (1992) 110:311–320

Contributions to Mineralogy and Petrology
© Springer-Verlag 1992

# Heat capacities of $Fe_2O_3$-bearing silicate liquids

**Rebecca A. Lange* and Alexandra Navrotsky**

Department of Geological and Geophysical Sciences, Princeton University, Princeton, NJ 08544, USA

Received April 26, 1991 / Accepted September 12, 1991

**Abstract.** Direct measurements of liquid heat capacity, using a Setaram HT1500 calorimeter in step-scanning mode, have been made in air on six compositions in the $Na_2O-FeO-Fe_2O_3-SiO_2$ system, two in the $CaO-FeO-Fe_2O_3-SiO_2$ system and four of natural composition (basanite, andesite, dacite, and peralkaline rhyolite). The fitted standard deviations on our heat capacity measurements range from 0.6 to 3.6%. Step-scanning calorimetry is particularly useful when applied to iron-bearing silicate liquids because: (1) measurements are made over a small temperature interval (10 K) through which the ferric-ferrous ratio of the liquid remains essentially constant during a single measurement; (2) the sample is held in equilibrium with an atmosphere that can be controlled; (3) heat capacity is measured directly and not derived from the slope of enthalpy measurements with temperature. Liquid compositions in the sodic and calcic systems were chosen because they contain large concentrations of $Fe_2O_3$ (up to 19 mol%), and their equilibrium ferric-ferrous ratios were known at every temperature of measurement. These measurements have been combined with heat capacity ($Cp$) data in the literature on iron-free silicate liquids to fit $Cp$ as a function of composition. A model assuming no excess heat capacity (linear combination of partial molar heat capacities of oxide components) reproduces the liquid data within error ($\pm 2.2\%$ on average). The derived partial molar heat capacity of the $Fe_2O_3$ component is 240.9 $\pm 7.9$ J/g.f.w.-K, with a standard error reduced by more than a factor of two from that in earlier studies. The model equation, based primarily on simple, synthetic compositions, predicts the heat capacity of the four magmatic liquids within 1.8% on average.

## Introduction

Heat capacity data on multicomponent silicate melts have two important applications in igneous petrology: (1) modelling the crystallization paths of evolving magmas (Ghiorso et al. 1983; Ghiorso and Carmichael 1985; Nekvasil 1988); (2) calculating the thermal evolution of cooling magma bodies (Jaeger 1968; Delaney 1988). The experimental goal, therefore, is to develop a model equation that describes the heat capacity of silicate melts over a wide range of composition. In order to be relevant to magmatic liquids, the model must extend to compositions that include both ferric and ferrous oxide components. Despite an expanding body of heat capacity data on silicate melts (Stebbins et al. 1982, 1983, 1984; Richet and Bottinga 1984a, b, 1985) the largest uncertainty is still associated with the ferric component (Stebbins et al. 1984). This can be attributed, in part, to the under-representation of liquids containing ferric iron in the data set (5 out of 55 compositions, 3 with $\leq 4$ mol% $Fe_2O_3$; Carmichael et al. 1977; Stebbins et al. 1984). Uncertainties also arise, however, from the inherent difficulty of accurately characterizing ferric and ferrous concentrations in silicate liquids during measurement of enthalpy by conventional drop calorimetry.

Prior to this study, heat capacities of stable and supercooled silicate liquids have not been measured directly but have been derived from drop calorimetric measurements of enthalpy as a function of temperature (e.g., Carmichael et al. 1977; Stebbins et al. 1984; Richet and Bottinga 1985). One of the difficulties with drop experiments applied to iron-bearing samples stems from the strong temperature dependence of the following reaction in silicate melts:

$$Fe_2O_3 = 1/2\,O_2 + 2\,FeO \quad (1)$$

At constant oxygen fugacity ($f\,O_2$), the reaction in Eq. (1) is driven to the right with increasing temperature; this strong temperature dependence affects the interpretation of drop calorimetric measurements on iron-bearing sam-

* *Present address:* Department of Geological Sciences, University of Michigan, Ann Arbor, MI 48109, USA

ples. In a typical experiment, a sample is equilibrated at some elevated temperature (for silicate liquids, typically between 1200–1800 K) and then dropped into a calorimetric block at room temperature, thus measuring $H_T - H_{298}$. The temperature interval over which a molten sample is dropped is often on the order of 1000 K, and if the sample is open to oxygen, its ferric-ferrous ratio will change during cooling. Alternatively, the sample can be loaded into a capsule and sealed with almost no air space such that changes in the ferric-ferrous ratio are small during the drop, although the oxygen fugacity of the sample is poorly defined. This latter approach is suitable for applications where accurate characterization of the sample $fO_2$ is unimportant. A more serious problem with drop experiments applied to fluid, iron-rich silicate melts is the tendency to form a mixture of crystalline phases or glass and crystals during the quench. Such experiments are extremely difficult to interpret because the standard-state thermodynamic properties of the quenched material (a mixture of solid-solution phases) are ill-defined. As a consequence, Carmichael et al. (1977) restricted their enthalpy measurements to relatively iron-poor (<4 mol% total $Fe_2O_3$) and silica-rich liquids that quench reproducibly to a glass.

The problems above can be minimized using a Setaram HT1500 calorimeter in step-scanning mode (Lange et al. 1991); in this approach, the change in enthalpy of a sample is measured during heating (or cooling) over a small temperature interval (typically 5 or 10 K), and thus provides a direct measurement of heat capacity. Over this small temperature interval, the ferric-ferrous ratio remains essentially constant during a single measurement. In addition, the samples are held in equilibrium with an atmosphere that can be controlled, allowing accurate characterization of the ferric-ferrous ratio in each sample at every temperature of measurement. This paper reports direct heat capacity measurements on six liquid compositions in the $Na_2O-FeO-Fe_2O_3-SiO_2$ system, two in the $CaO-FeO-Fe_2O_3-SiO_2$ system and four of natural composition (basanite, andesite, dacite, rhyolite), all in equilibrium with air. These measurements are combined with heat capacity data in the literature on iron-free multicomponent silicate melts (Naylor 1945; King et al. 1954; Carmichael et al. 1977; Richet and Bottinga 1980, 1984a, b, 1985; Richet et al. 1984; Stebbins et al. 1982, 1983, 1984) to develop a model equation applicable to liquids of magmatic composition.

## Experimental methods

### *Starting materials*

Six compositions in the $Na_2O-FeO-Fe_2O_3-SiO_2$ system and two compositions in the $CaO-FeO-Fe_2O_3-SiO_2$ system were

**Table 1.** Compositions (mol%) and measured heat capacities (J/g.f.w.-K) of sodic and calcic liquids

| Sample | $T$ (K) | $SiO_2$ | $Fe_2O_3$ | FeO | CaO | $Na_2O$ | $Cp^{meas}$ | [a] $Cp^{calc}$ |
|---|---|---|---|---|---|---|---|---|
| CFS-A | 1532 | 53.84 | 10.23 | 4.42 | 31.51 | – | 107.50 | 100.91 |
| CFS-A | 1607 | 53.44 | 9.41 | 5.88 | 31.27 | – | 106.71 | 99.53 |
| CFS-B | 1607 | 35.19 | 15.40 | 4.69 | 44.72 | – | 110.29 | 110.02 |
| CFS-B | 1651 | 35.03 | 14.90 | 5.54 | 44.53 | – | 108.70 | 109.18 |
| NFS-1 | 1140 | 43.39 | 18.75 | 0.03 | – | 37.83 | 113.09 | 117.98 |
| NFS-1 | 1235 | 43.38 | 18.71 | 0.09 | – | 37.82 | 118.98 | 117.91 |
| NFS-2 | 1140 | 51.28 | 12.68 | 0.02 | – | 36.02 | 108.33 | 108.10 |
| NFS-2 | 1235 | 51.26 | 12.65 | 0.07 | – | 36.01 | 105.51 | 108.04 |
| NFS-2 | 1329 | 51.23 | 12.58 | 0.20 | – | 35.99 | 108.60 | 107.93 |
| NFS-2 | 1424 | 51.16 | 12.43 | 0.47 | – | 35.94 | 105.02 | 107.67 |
| NFS-2 | 1519 | 51.02 | 12.12 | 1.01 | – | 35.84 | 102.90 | 107.14 |
| NFS-2 | 1614 | 50.77 | 11.57 | 1.99 | – | 35.67 | 104.19 | 106.21 |
| NFS-4 | 1235 | 59.71 | 9.45 | 0.06 | – | 30.79 | 99.90 | 102.21 |
| NFS-4 | 1329 | 59.68 | 9.39 | 0.16 | – | 30.77 | 104.95 | 102.10 |
| NFS-4 | 1519 | 59.48 | 9.03 | 0.82 | – | 30.67 | 107.31 | 101.49 |
| NFS-4 | 1614 | 59.25 | 8.60 | 1.60 | – | 30.55 | 104.32 | 100.76 |
| NFS-5 | 1233 | 66.95 | 4.50 | 0.03 | – | 28.52 | 98.26 | 94.03 |
| NFS-5 | 1327 | 66.93 | 4.47 | 0.08 | – | 28.51 | 94.41 | 93.97 |
| NFS-5 | 1422 | 66.89 | 4.41 | 0.20 | – | 28.50 | 92.41 | 93.87 |
| NFS-5 | 1517 | 66.82 | 4.29 | 0.43 | – | 28.46 | 97.38 | 93.67 |
| NFS-5 | 1612 | 66.68 | 4.08 | 0.83 | – | 28.41 | 91.00 | 93.31 |
| NFS-6 | 1233 | 66.96 | 8.63 | 0.06 | – | 24.36 | 101.05 | 99.95 |
| NFS-6 | 1327 | 66.92 | 8.58 | 0.15 | – | 24.35 | 103.90 | 99.85 |
| NFS-6 | 1422 | 66.85 | 8.46 | 0.36 | – | 24.32 | 100.76 | 99.64 |
| NFS-6 | 1517 | 66.72 | 8.24 | 0.77 | – | 24.27 | 99.84 | 99.28 |
| NFS-6 | 1612 | 66.47 | 7.84 | 1.50 | – | 24.18 | 99.16 | 98.60 |
| NFS-8 | 1238 | 78.48 | 9.60 | 0.07 | – | 11.85 | 100.65 | 99.60 |
| NFS-8 | 1291 | 78.46 | 9.57 | 0.12 | – | 11.85 | 99.01 | 99.55 |
| NFS-8 | 1343 | 78.43 | 9.53 | 0.20 | – | 11.84 | 102.99 | 99.48 |
| NFS-8 | 1395 | 78.38 | 9.46 | 0.33 | – | 11.83 | 96.37 | 99.37 |
| NFS-8 | 1447 | 78.31 | 9.36 | 0.51 | – | 11.82 | 96.46 | 99.20 |
| NFS-8 | 1500 | 78.21 | 9.21 | 0.78 | – | 11.81 | 99.10 | 98.96 |
| NFS-8 | 1552 | 78.06 | 9.01 | 1.14 | – | 11.78 | 100.35 | 98.61 |

[a] Calculated using the model of this study presented in Table 4

**Table 2.** Compositions (mol%) and measured heat capacities (J/g.f.w.-K) of the natural samples

| Sample | $T$(K) | $SiO_2$ | $TiO_2$ | $Al_2O_3$ | $Fe_2O_3$ | FeO | MgO | CaO | $Na_2O$ | $K_2O$ | $Cp^{meas}$ | $^aCp^{calc}$ |
|---|---|---|---|---|---|---|---|---|---|---|---|---|
| Basanite | 1535 | 48.15 | 2.23 | 10.24 | 3.78 | 1.53 | 15.60 | 14.24 | 3.22 | 1.01 | 102.31 | 101.59 |
| Basanite | 1594 | 48.05 | 2.22 | 10.22 | 3.58 | 1.91 | 15.57 | 14.21 | 3.22 | 1.01 | 103.12 | 101.23 |
| Basanite | 1637 | 47.98 | 2.22 | 10.21 | 3.42 | 2.21 | 15.55 | 14.19 | 3.21 | 1.01 | 100.63 | 100.96 |
| Basanite | 1674 | 47.92 | 2.22 | 10.19 | 3.28 | 2.47 | 15.53 | 14.17 | 3.21 | 1.01 | 103.44 | 100.70 |
| Andesite | 1492 | 56.81 | 0.24 | 9.84 | 3.22 | 1.40 | 12.37 | 13.21 | 2.48 | 0.42 | 98.64 | 99.17 |
| Andesite | 1535 | 56.71 | 0.24 | 9.82 | 3.04 | 1.75 | 12.35 | 13.19 | 2.47 | 0.42 | 102.12 | 98.85 |
| Andesite | 1594 | 56.64 | 0.24 | 9.81 | 2.91 | 2.01 | 12.33 | 13.17 | 2.47 | 0.42 | 100.41 | 98.63 |
| Andesite | 1637 | 56.57 | 0.24 | 9.80 | 2.78 | 2.25 | 12.32 | 13.15 | 2.47 | 0.42 | 96.72 | 98.40 |
| Dacite | 1468 | 69.04 | 0.56 | 11.64 | 1.83 | 0.58 | 3.86 | 6.44 | 5.15 | 0.89 | 100.32 | 97.67 |
| Dacite | 1510 | 69.00 | 0.56 | 11.63 | 1.77 | 0.70 | 3.86 | 6.44 | 5.15 | 0.89 | 98.59 | 97.57 |
| Dacite | 1551 | 68.96 | 0.56 | 11.62 | 1.71 | 0.82 | 3.86 | 6.43 | 5.15 | 0.89 | 95.13 | 97.46 |
| Dacite | 1593 | 68.91 | 0.56 | 11.61 | 1.64 | 0.96 | 3.86 | 6.43 | 5.14 | 0.88 | 95.71 | 97.33 |
| Pantellerite | 1437 | 76.47 | 0.42 | 8.01 | 2.38 | 0.56 | 0.22 | 0.61 | 7.58 | 3.76 | 94.12 | 95.32 |
| Pantellerite | 1489 | 76.41 | 0.42 | 8.00 | 2.31 | 0.71 | 0.22 | 0.61 | 7.57 | 3.75 | 97.43 | 95.18 |
| Pantellerite | 1541 | 76.34 | 0.42 | 8.00 | 2.22 | 0.89 | 0.22 | 0.61 | 7.57 | 3.75 | 94.41 | 95.05 |
| Pantellerite | 1593 | 76.27 | 0.42 | 7.99 | 2.12 | 1.08 | 0.22 | 0.61 | 7.56 | 3.75 | 98.17 | 94.88 |

[a] Calculated using the model of this study presented in Table 4

chosen for calorimetric measurements (Tables 1 and 2). The method of preparation and quality control on composition and homogeneity have been discussed in detail by Lange and Carmichael (1989) and Kress and Carmichael (1989). Liquid compositions in these two systems were chosen because they contain large concentrations of $Fe_2O_3$ (up to 19 mol%), and their equilibrium ferric-ferrous ratios in air can be calculated accurately from the calibrated equations of Lange and Carmichael (1989) and Kress and Carmichael (1989). Thus, the mole fraction of ferric and ferrous iron were determined in each experimental liquid at every temperature of measurement. Moreover, the low liquidus temperatures of the $Na_2O-FeO-Fe_2O_3-SiO_2$ samples (850–950° C) allowed a wide temperature range in the *liquid* state to be accessed by calorimetry; this gave an opportunity to explore the temperature dependence to the heat capacity of $Fe_2O_3$-bearing silicate melts. Four natural silicate melts also were chosen for calorimetric measurements: an andesite from Manam Island, a basanite from the Korath range in Uganda, a dacite from Mt. St. Helens, Washington, and a peralkaline rhyolite from Pantelleria, Italy. The ferric-ferrous ratios of these natural silicate liquids in equilibrium with air at every temperature of measurement were calculated using the calibration equation of Kress and Carmichael (1988).

## *Calorimetric procedures*

Calorimetric measurements were made in a Setaram HT1500 calorimeter in step-scanning mode. Because the apparatus and experimental procedure have been described in detail by Lange et al. (1991), only a brief summary is presented here. The calorimetric detector consists of an upper and lower thermopile surrounding a sample and reference chamber respectively. In our experiments, the reference chamber held an alumina crucible filled with dried corundum powder, whereas the sample chamber held an alumina crucible with a tight-fitting 95% Pt-5% Au inner capsule with a Pt-foil lid. The inner Pt–Au capsule was either empty (a blank), filled with tamped corundum powder (a calibration), or filled with an iron-bearing silicate melt (a sample). Care was taken to ensure that the *volume* of melt in each sample run was equivalent to the *volume* of corundum used in the calibration runs.

Before calorimetry on each iron-bearing sample, that composition was pre-loaded into a new 95% Pt-5% Au inner calorimeter capsule and fused in a box furnace in air above its liquidus for 24 h. The capsule was then cleaned with HF and a fresh batch of sample was re-loaded into the same Pt–Au capsule. This pre-saturation procedure, combined with the fact that the calorimetric measurements were performed in air, minimized iron loss from the sample to the Pt–Au capsule. Analyses of each sample before and after the calorimetric measurements (using the JEOL 8600 electron microprobe at Rutgers University) are presented in Appendix 1 and confirm that virtually no iron loss took place. Soda loss was restricted to less than 2 wt% for the sodic samples, probably because the liquids were enclosed in capsules with Pt-foil lids during the experiment. Pt–Au capsules were used to minimize wetting and creep of iron-bearing silicate melts, a problem with pure Pt.

During an experiment, the calorimetric detector sat inside an alumina tube (within a graphite tube furnace) where the atmosphere could be controlled; in this study, all measurements were made in air. A scanning experiment consisted of three runs: a blank, a calibration, and a sample. Before each sample run, the furnace was taken to the lowest experimental temperature, and the ferric-ferrous ratio of the sample was allowed to equilibrate for 24 h. During a scanning run, the thermopile voltage was monitored as the temperature was raised (or lowered) at a rate of 1 K/min over a temperature interval of 10 K. A 10 min heating (or cooling) period

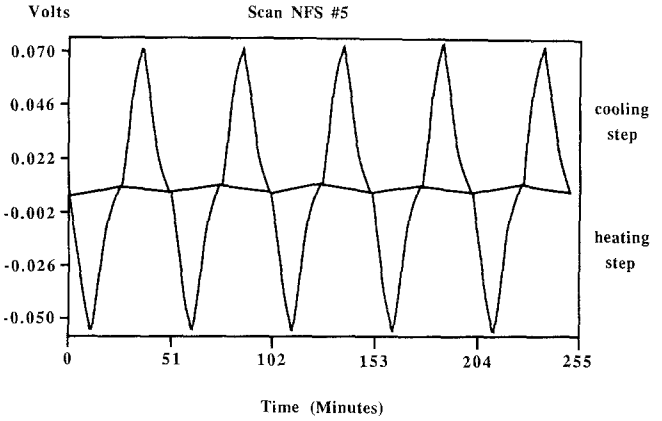


**Fig. 1.** Typical plot of voltage vs time during ten alternating heating and cooling scanning steps. In this example, the sodic melt initially was heated at a rate of 1 K/min for 10 min followed by an isothermal interval of 15 min. The melt was then cooled at a rate of 1 K/min for 10 min followed by another isothermal period. This cycle was repeated five times. The area under each peak was calculated and the average of the ten values was taken as one data point

was followed by a 15 min isothermal period to equilibrate the calorimeter. A typical run consisted of ten alternating heating and cooling steps (Fig. 1); the average of the integrated areas under ten voltage peaks represents one datum point. The results of the blank runs were subtracted from those of the calibration and sample runs, and corrections were applied for the small differences in weight between the different Pt–Au crucibles. Data were reduced using the following relationship:

$$Cp(T)_{\text{sample}} = [(A/\Delta T)_{\text{sample}} - (A/\Delta T)_{\text{blank}})](\gamma M_s/m_s) \quad (2)$$

where $T=(T_2+T_1)/2$ and $T_2$ and $T_1$ bracket the scanning temperature interval (10 K) $\Delta T = T_2 - T_1$
$M_s$ = molecular weight of the silicate melt sample
$m_s$ = mass of the silicate melt sample
$A$ = integrated area under voltage peak (average of 10 peaks)
and

$$\gamma(\text{calibration factor}) = [(m_{Al_2O_3} Cp(T)_{Al_2O_3}/M_{Al_2O_3}]/[(A/\Delta T)_{Al_2O_3} - (A/\Delta T)_{\text{blank}}] \quad (3)$$

where $Cp(T)_{Al_2O_3}$ = heat capacity of corundum from Robie et al. (1978)
$m_{Al_2O_3}$ = mass of corundum
$M_{Al_2O_3}$ = molecular weight of corundum.

The calibration factors increased as the temperature of the experiments increased, indicating a decrease in sensitivity with increasing temperature. This is probably due to an increase in the transfer of heat by radiation relative to the heat transferred by conduction through the thermopiles at high temperature. As a consequence, measurements were restricted to temperatures < 1700 K. Temperature was measured with a Pt-6% Rh/Pt-30% Rh thermocouple located next to the sample chamber. The calibration of this thermocouple was checked by melting a gold sample (1337 K) in the alumina sample chamber.

## Results

Heat-capacity measurements on the $Na_2O-FeO-Fe_2O_3-SiO_2$ liquids are presented in Table 1. Twenty-nine measurements were made on liquids containing between 4.08 and 18.75 mol% $Fe_2O_3$. The low liquidus temperatures of these compositions allowed measurements to be made over a range of 300–400 K. The single exception is composition no. 1; the experiments above 1300 K were discarded because the capsule leaked at high temperatures. Also seen in Table 1 are the mole fractions of $Fe_2O_3$ in the melts at the lowest and highest temperatures of measurement. In all cases, the change in $Fe_2O_3$ (reflecting variation in the ferric-ferrous ratio with temperature) is $\leq 1$ mol% over the experimental temperature range. Within the error of the measurements, no temperature dependence to the liquid heat capacities could be resolved.

Only two compositions in the $CaO-FeO-Fe_2O_3-SiO_2$ system had sufficiently low liquidus temperatures such that they could be used for calorimetric measurements. The results for these melts as well as those for the natural liquids are presented in Tables 1 and 2. Measurements were only possible in the stable liquid region due to rapid crystallization below the liquidus. This severely limited the temperature range over which measurements could be made (< 150 K) and no temperature dependence to $Cp$ was resolved for any of the samples. Because of the limited temperature range of the measurements, the change in $Fe_2O_3$ in the experimental melts (variation in the ferric-ferrous ratio with temperature) was always $\leq 1$ mol%.

### *Experimental precision and accuracy*

The ten alternating heating and cooling steps during each run (Fig. 1) allow an average integrated area under the voltage peak to be calculated (with its standard deviation) at each temperature of measurement. The standard deviations on $A_{\text{blank}}$, $A_{Al_2O_3}$ and $A_{\text{sample}}$ in Eqs. 2, 3 lead to a propagated error on $Cp_{\text{sample}}$ that varies from 5–10%. However, the *fitted* standard deviation on $Cp_{\text{sample}}$ for each melt composition (assuming no temperature dependence) is much smaller (Table 3). Although the procedure for calculating the standard deviation ignores changes in the ferric-ferrous ratios of the melts with temperature, it does provide a measure of the precision of the step-scanning method that can be compared directly to that reported for heat capacity data in the literature derived by differentiating enthalpy data. The

**Table 3.** Mean heat capacity and standard deviation for each composition

| Sample | $\Delta T$[a] (K) | $\Delta Fe_2O_3$[a] (mol%) | $Cp$ (J/g.f.w.-K) | S.D.[b] | S.D./mean (×100) |
|---|---|---|---|---|---|
| NFS-1 | 95 | 0.04 | 116.04 | 4.16 | 3.6% |
| NFS-2 | 474 | 1.11 | 105.76 | 2.28 | 2.2% |
| NFS-4 | 285 | 0.79 | 105.41 | 3.09 | 2.9% |
| NFS-5 | 379 | 0.42 | 93.51 | 3.12 | 3.3% |
| NFS-6 | 379 | 0.79 | 100.94 | 1.82 | 1.8% |
| NFS-8 | 314 | 0.59 | 99.28 | 2.36 | 2.4% |
| CFS-A | 75 | 0.82 | 107.11 | 0.56 | 0.5% |
| CFS-B | 44 | 0.50 | 109.62 | 1.12 | 1.0% |
| Basanite | 139 | 0.50 | 102.38 | 1.26 | 1.2% |
| Andesite | 145 | 0.44 | 99.47 | 2.32 | 2.3% |
| Dacite | 125 | 0.19 | 97.44 | 2.45 | 2.5% |
| Pantellerite | 156 | 0.26 | 96.03 | 2.07 | 2.2% |

[a] Difference in $T$ and $X_{Fe_2O_3}$ between lowest and highest temperature of $Cp$ measurement
[b] S.D., standard deviation about the mean

**Table 4.** Fitted partial molar liquid oxide heat capacities

| | $Cp(\text{liq}) = \sum X_i Cp_i$(J/g.f.w.-K) | |
|---|---|---|
| Oxide | $Cp_i \pm 1\sigma$ (This study)[a] | $Cp_i \pm 1\sigma$ Stebbins et al. (1984)[b] |
| $SiO_2$ | 82.6 ± 1.2 | 80.0 ± 0.9 |
| $TiO_2$ | 109.2 ± 8.9 | 111.8 ± 5.1 |
| $Al_2O_3$ | 170.3 ± 5.1 | 157.6 ± 3.4 |
| $Fe_2O_3$ | 240.9 ± 7.9 | 229.0 ± 18.4 |
| FeO | 78.8 ± 4.6 | 78.9 ± 4.9 |
| MgO | 94.2 ± 4.3 | 99.7 ± 7.3 |
| CaO | 89.8 ± 3.1 | 99.9 ± 7.2 |
| $Na_2O$ | 97.6 ± 3.1 | 102.3 ± 1.9 |
| $K_2O$ | 98.5 ± 5.5 | 97.0 ± 5.1 |

[a] Unweighted regression
[b] Weighted regression based on experimental precision

reported precision (e.g., Stebbins et al. 1982, 1983, 1984; Richet and Bottinga 1984a, b, 1985) is the *fitted* error on the coefficient $b$, based on the regression equation: $H_T - H_{298} = a + bT$, where $b = Cp$ and in many cases is independent of temperature. For example, Stebbins et al. (1984) report standard errors on their heat-capacity data that range from 1 to 3% of the estimate, whereas Richet and Bottinga (1985) have standard errors that range from 0.1 to 0.6% of the estimate. The fitted standard deviations on our heat-capacity measurements range from 0.6 to 3.6% (Table 4). Our assessment of the accuracy of the technique is based on our heat-capacity measurements on the $Na_2Si_2O_5$ melt composition (Table 1). The heat capacity of this liquid has been measured with a very high precision ($\pm 0.5\%$) by Richet et al. (1984); our measurement is within 1.7% of their reported value, indicating good interlaboratory agreement.

*Previous measurements on iron-bearing silicate liquids*

The first drop calorimetric measurements on iron-bearing silicate liquids were made by Carmichael et al. (1977) on three natural samples (a rhyolite, an andesite, and a peralkaline rhyolite). These liquids contained 0.80, 4.24, and 3.89 mol% $Fe_2O_3$ (total iron) respectively. Efforts were made to ensure that all of the iron was oxidized to $Fe_2O_3$ by holding each composition open to the atmosphere at 800 K for 24 h before the containers were crimped shut. However, for the reasons outlined in the introduction, there is some uncertainty as to what ferric-ferrous ratio should be assigned to these liquids. Given the low total iron contents of these melts, this probably does not affect significantly the derived heat-capacity data. At the same time, however, because of the low $Fe_2O_3$ concentrations, heat-capacity measurements on these melts provide only weak constraints on the partial molar heat capacity of $Fe_2O_3$.

The second set of calorimetric measurements on iron-bearing silicate liquids were made by Stebbins et al. (1984) on $NaFeSi_3O_8$ and $KFeSi_3O_8$ melt compositions. To control the ferric-ferrous ratios in the melts during drop experiments, the samples were first equilibrated in air in open Pt-10% Rh capsules at the highest temperature to be reached during calorimetry. The capsules were then filled with argon and sealed by welding. Constant composition was believed to be maintained at lower temperatures because additional oxygen was not available to raise the ratio of ferric to ferrous iron; that is, the $fO_2$ in the capsule adjusted to the constant liquid composition. The $NaFeSi_3O_8$ and $KFeSi_3O_8$ melts were reported to contain 9.08 and 8.88 mol% $Fe_2O_3$ respectively.

Stebbins et al. (1984) derived a value for the partial molar heat capacity of the $Fe_2O_3$ component ($Cp_{Fe_2O_3}$) of $229.0 \pm 18.0$ J/g.f.w.-K that is based on their two measurements on iron-bearing samples in addition to those of Carmichael et al. (1977) on the three natural samples. Richet and Bottinga (1985), on the other hand, derived a value for $Cp_{Fe_2O_3}$ of 199.7 J/g.f.w.-K that is based only on the two measurements of Stebbins et al. (1984). Given the discrepancy between the two reported values, we have taken our 33 measurements on the sodic and calcic silicate melts, 27 of which contain between 8 and 19 mol% $Fe_2O_3$, and have fitted a new value for the partial molar heat capacity of $Fe_2O_3$ in silicate melts. The calibration of our regression equation is described below.

## Discussion

*Calibration of a model equation*

Currently, there are two model equations in the literature that describe the heat capacities of multicomponent silicate liquids. The first is that of Stebbins et al. (1984):

$$Cp^{liq} = \sum X_i Cp_i \tag{4}$$

where $X_i$ is the mole fraction of oxide component $i$ and $Cp_i$ is the partial molar heat capacity of component $i$. Implicit in this equation are two assumptions, namely that the partial molar heat capacity of each oxide component is independent of composition and temperature. In detail, it is known that this is not strictly true; significant non-linearity in mixing is observed in simple systems (e.g., $CaMgSi_2O_6 - NaAlSi_3O_8$) and both a negative and positive temperature dependence to liquid heat capacities have been observed for some compositions (Stebbins et al. 1984; Richet and Bottinga 1984a, 1985). However, Stebbins et al. (1984) found that calibration of a general model equation on all available liquid $Cp$ data [primarily from two research groups: (1) Stebbins and Carmichael at Berkeley; (2) Richet and Bottinga in France] did not lead to any temperature-dependent or non-linear compositional terms that were statistically significant.

In contrast to the simple model of Stebbins et al. (1984), Richet and Bottinga (1985) present a more complex model equation of the form:

$$Cp^{liq}(T) = \sum X_i Cp_i(T) + X_{K_2O} X_{SiO_2} W_{KS} \tag{5}$$

where $Cp_{Al_2O_3}$, $Cp_{TiO_2}$ and $Cp_{K_2O}$ have a temperature dependence and $W_{KS}$ is an interaction parameter between the $K_2O$ and $SiO_2$ components. Their model equation is calibrated on a much smaller set of heat capacity data on liquids without alumina. The coefficient for $Al_2O_3$ is estimated independently from data on a few aluminous compositions. The model of Richet and Bottinga (1985) is an attempt to include the complexities in $Cp$ with temperature and composition that have been documented in some simple 3- and 4-component silicate liquids. However, the question remains whether the complexities observed in these simple systems can be extrapolated to multicomponent liquids of magmatic composition.

Another factor to consider during calibration of a model $Cp$ equation is the distinction between the precision and accuracy of heat capacity data, including systematic differences among precise measurements made in different laboratories. An opportunity to evaluate these factors is found with the published heat capacity

data on liquid albite ($NaAlSi_3O_8$) from four separate studies (Richet and Bottinga 1980, 1984a; Stebbins et al. 1982; Navrotsky et al. 1989). Enthalpies of stable- and supercooled-liquid albite have been measured in two studies by Richet and Bottinga (1980, 1984a). The first set of enthalpy measurements by Richet and Bottinga (1980) was made on melted natural albite crystals from Mondane (French Alps). The enthalpy data on liquid albite (1166–1486 K) were fitted to the following equation:

$$H_T - H_{298} = a + bT \quad (6)$$

where $Cp = b$ (independent of temperature) and has a derived value of $89.38 \pm 0.36$ J/g.f.w.-K. The fitted standard error on $Cp$ is only 0.4% of the estimate and reflects the high precision of the enthalpy measurements. In the second study, Richet and Bottinga (1984a) used a different albite sample, a glass synthesized by D.F. Weill (see Weill et al. 1980), and they point out a significant difference between the glass transition temperatures ($Tg$ of 1158 K and 1096 K for the natural and synthetic samples respectively), leading to a systematic difference of about 1.6 kJ/mole in the enthalpy reported in the two studies. However, Richet and Bottinga (1984a) stress that the enthalpy-temperature relationships in the liquid range are quite similar in both studies and that the difference in $Tg$ did not affect the derived $Cp$. They fitted their enthalpy measurements on the synthetic liquid albite (between 1096–1791 K) to the following model equation:

$$H_T - H_{298} = a + bT + cT^2/2, \quad (7)$$

that implies a temperature dependence to the liquid heat capacity. However, if the enthalpy data of Richet and Bottinga (1984a) are fitted to the more simple model in Eq. 6, the derived value of $Cp(=b)$ is $90.41 \pm 0.34$. Again, the fitted standard error on $Cp$ is only 0.4% which is well within the experimental uncertainty in $Cp$ of $\pm 0.5\%$ reported by Richet and Bottinga (1984a). Any temperature dependence to the heat capacity of liquid albite does not, therefore, appear to be justified by the experimental data. The two $Cp$ values for liquid albite derived from the two studies differ by 1.1%; this probably provides a good estimate of the reproducibility (vs the fitted precision) of the measurements.

The same albite sample synthesized by Weill was also used in the drop calorimetric measurements of Stebbins et al. (1982). Their measurements were performed over a more narrow temperature interval (1457–1810 K) in the stable-liquid region only. The enthalpy measurements were fitted to the model in Eq. 6, leading to a derived $Cp$ value of $92.96 \pm 0.77$ J/g.f.w.-K. The slightly larger standard error on $Cp$ of 0.8%, relative to the two studies of Richet and Bottinga, reflects the smaller temperature interval over which enthalpy measurements were made and not the precision of the enthalpy measurements. The heat capacity of liquid albite reported by Stebbins et al. (1982) is within 2.7% of the value determined from the data of Richet and Bottinga (1984a); this provides a good estimate of interlaboratory errors, despite the fact that the enthalpy measurements in all three studies are extremely precise (0.2–0.5%). The fourth study on the heat capacity of liquid albite was performed by transposed-temperature drop calorimetry by Navrotsky et al. (1989), where the sample was dropped from room temperature into a calorimetric detector at high temperature. Their enthalpy measurements on an albite specimen from the Franciscan vein (described by Apps and Neil 1978) were fitted to Eq. 6, leading to a derived value for $Cp$ of $92.08 \pm 2.85$ J/g.f.w.-K. This value is within 1.8% and 1.0% respectively of those reported by Richet and Bottinga (1984a) and Stebbins et al. (1984).

Both Stebbins et al. (1984) and Richet and Bottinga (1985) used $Cp$ data published from *both* of their laboratories to calibrate their respective $Cp$ models. It is difficult, in fact, to develop a comprehensive $Cp$ model applicable to natural silicate liquids without using the extensive data of both research groups. As a consequence, any model calibrated on both data sets that reproduces the $Cp$ measurements within 2–3% is within the interlaboratory errors. With this in mind, we have combined our heat capacity measurements on the sodic, calcic, and natural iron-bearing liquids (Tables 1 and 2) with $Cp$ data in the literature on 41 iron-free silicate melts (Naylor 1945; King et al. 1954; Richet and Bottinga 1980, 1984a, b, 1985; Richet et al. 1984, 1990; Stebbins et al. 1982, 1983, 1984) to calibrate the following regression equation:

$$Cp = \sum X_i Cp_i \quad (8)$$

where $X_i$ is the mole fraction of each oxide component $i$, and $Cp_i$ is the partial molar heat capacity of each oxide component $i$ and is independent of temperature and composition. Liquids that are *not* included in our regression are three alkali-titania silicate melts (one from Carmichael et al. 1977 and two from Richet and Bottinga 1985) that exhibit a pronounced negative temperature dependence to their heat capacities. These compositions were excluded as there is evidence from density measurements (Lange and Carmichael 1987; Johnson 1990) that $Ti^{4+}$ exists in more than one coordination (4-, 5- and 6-fold) in alkali silicate melts but occurs primarily in octahedral coordination in alkaline-earth silicate and *natural* melts (Lange and Carmichael 1990). In addition, the heat capacity measurement on fayalite ($Fe_2SiO_4$) liquid (in an Fe-plated capsule) by Stebbins and Carmichael (1984) is also included in our final data set. A detailed description of the liquid composition and its ferric-ferrous ratio during the calorimetric experiments is found in Stebbins and Carmichael (1984).

### *Regression results*

The results of our unweighted regression, based on 88 liquid heat capacity measurements, are presented in Table 4; the average deviation between calculated and measured heat capacities is 2.3%. In Tables 1 and 2, the difference between calculated and measured heat capacities can be directly compared; note how little the effect of temperature-induced compositional change (ferric-ferrous ratio) has on the calculated $Cp$ values. The differ-

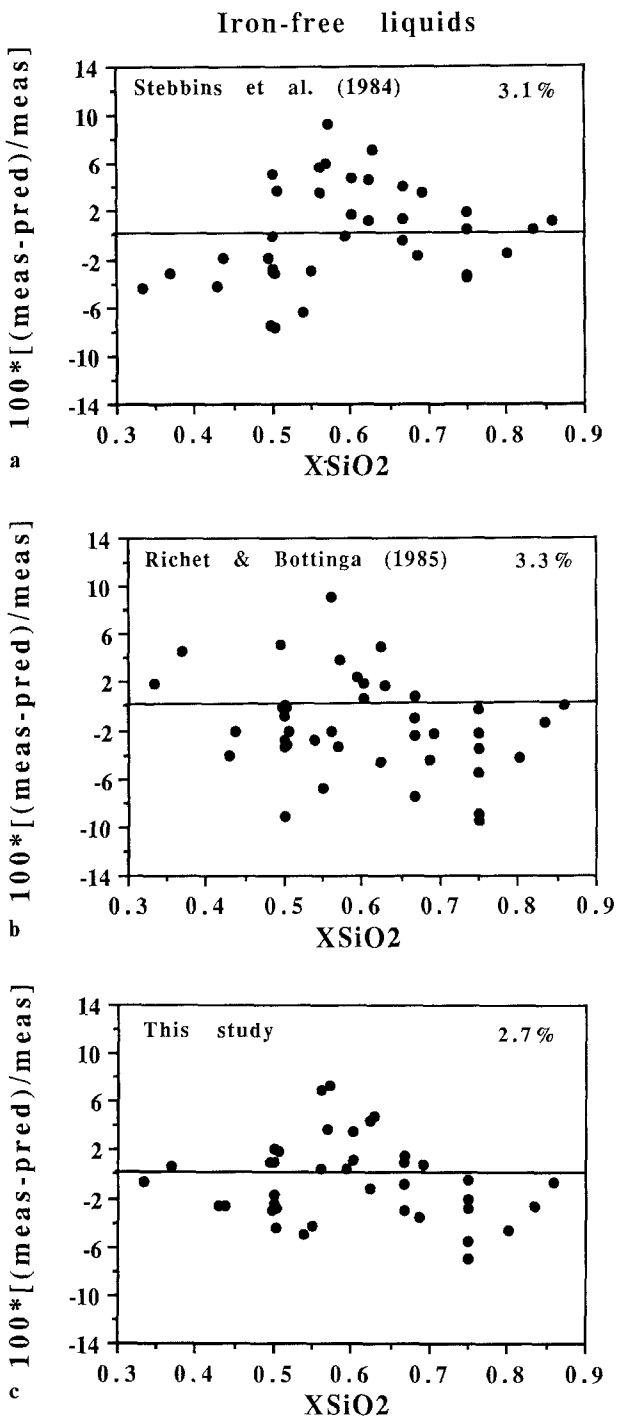


**Fig. 2a–c.** A plot of normalized residuals vs mole fraction of silica for the 41 iron-free silicate melts from the literature used to calibrate the *Cp* model of this study. The residuals correspond to the differences between the measured heat capacities and those calculated from the models of: **a** Stebbins et al. (1984); **b** Richet and Bottinga (1985); **c** this study

ences between the measured heat capacities on the 41 *iron-free* silicate liquids and those calculated from the models of (a) Stebbins et al. (1984); (b) Richet and Bottinga (1985); (c) this study, are plotted in Fig. 2. Our model reproduces the measured heat capacities of the *iron-free* melts within 2.7% on average while those of Stebbins et al. (1984) and Richet and Bottinga (1985) reproduce

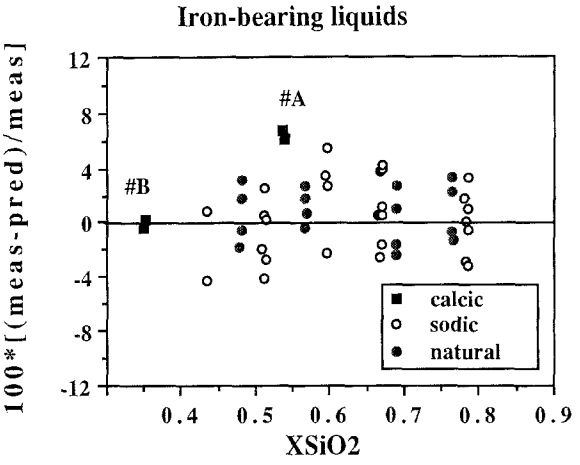


**Fig. 3.** A plot of normalized residuals vs mole fraction of silica for the iron-bearing liquids. Note that the largest residual is associated with composition CFS-A. Both liquid density data (Dingwell and Brearley 1988) and glass Mössbauer data (Morinaga et al. 1976; Iwamoto et al. 1978) suggest that this liquid may contain both tetrahedral and octahedral ferric iron

the 41 measurements within 3.1% and 3.3% respectively. Our fitted partial molar heat capacity values for each of the oxide components are compared in Table 4 to those derived from the weighted regression of Stebbins et al. (1984); the regression equations in both studies are identical. Our fitted partial molar heat capacity for the $Fe_2O_3$ component has a value of $240.9 \pm 7.9$ J/g.f.w.-K, with a standard error that has been reduced by more than a factor of two from that reported by Stebbins et al. (1984). Our model reproduces the iron-bearing silicate liquid heat-capacity measurements within 2.1% on average. The largest residual is associated with composition CFS-A which has measured heat capacities that deviate by 6.1 and 6.7% from the predicted values (Fig. 3). The other calcic composition (CFS-B) has measured heat capacities that differ by 0.2 and 0.4% from those calculated by the model.

### *Evidence for multiple $Fe^{3+}$ coordination in the melt?*

Interest in the heat capacity behavior of these two calcic melts, especially relative to the sodic melts, is sparked by Mössbauer spectroscopic evidence that $Fe^{3+}$ occupies more than one coordination environment in calcic silicate glasses (Iwamoto et al. 1978; Bowker et al. 1981). Specifically, Pargamin et al. (1972) noted that ferric iron is entirely four-fold coordinated in $Na_2O-FeO-Fe_2O_3-SiO_2$ glasses, while it occupies both octahedral and tetrahedral sites in $CaO-FeO-Fe_2O_3-SiO_2$ glasses. This observation is consistent with the liquid-density measurements of Dingwell et al. (1988) and Dingwell and Brearley (1988) in that the partial molar volume of $Fe_2O_3$ is independent of composition in sodic silicate melts but is strongly dependent on the $X_{CaO}$: $X_{SiO_2}$ ratio in calcic silicate melts (Lange and Carmichael 1990: Fig. 1). This is further supported by the Mössbauer studies of Morinaga et al. (1976) and Iwamoto et al. (1978) that both report an increase in the propor-

**Appendix 1a.** Electron microprobe analyses of sodic and calcic glass samples

| Sample | | $SiO_2$ (wt%) | $FeO^{total}$ (wt%) | CaO (wt%) | $Na_2O$ (wt%) | Total[a] |
|---|---|---|---|---|---|---|
| CFS-A | Pre-run | 46.74 (0.53) | 25.84 (0.21) | 25.63 (0.19) | – | 98.21 |
| CFS-A | Post-run | 46.82 (0.44) | 25.95 (0.27) | 25.98 (0.21) | – | 98.75 |
| CFS-B | Pre-run | 28.41 (0.50) | 34.51 (0.18) | 33.72 (0.28) | – | 96.64 |
| CFS-B | Post-run | 28.70 (0.48) | 34.62 (0.17) | 34.85 (0.24) | – | 98.17 |
| NFS-1 | Pre-run | 32.80 (0.51) | 33.92 (0.21) | – | 29.50 (0.24) | 96.22 |
| NFS-1 | Post-run | 33.86 (0.38) | 35.25 (0.19) | – | 27.82 (0.32) | 96.95 |
| NFS-2 | Pre-run | 41.98 (0.48) | 24.84 (0.19) | – | 30.42 (0.19) | 97.24 |
| NFS-2 | Post-run | 42.22 (0.55) | 25.42 (0.13) | – | 29.67 (0.22) | 97.29 |
| NFS-4 | Pre-run | 51.18 (0.50) | 19.44 (0.20) | – | 27.22 (0.17) | 97.84 |
| NFS-4 | Post-run | 50.14 (0.45) | 20.94 (0.17) | – | 26.77 (0.21) | 97.86 |
| NFS-5 | Pre-run | 61.83 (0.52) | 9.90 (0.14) | – | 27.17 (0.25) | 98.90 |
| NFS-5 | Post-run | 62.40 (0.49) | 10.32 (0.10) | – | 26.47 (0.13) | 99.17 |
| NFS-6 | Pre-run | 58.17 (0.44) | 17.99 (0.16) | – | 21.83 (0.18) | 97.99 |
| NFS-6 | Post-run | 57.93 (0.43) | 18.44 (0.10) | – | 21.63 (0.13) | 98.01 |
| NFS-8 | Pre-run | 67.49 (0.52) | 19.80 (0.19) | – | 10.51 (0.17) | 97.80 |
| NFS-8 | Post-run | 67.16 (0.44) | 20.21 (0.12) | – | 10.21 (0.11) | 97.57 |

Standard deviations indicated in parentheses

[a] Totals are low because most of the iron in all of the samples is ferric

**Appendix 1b.** Electron microprobe analyses of the natural glass samples

| Sample | | $SiO_2$ (wt%) | $TiO_2$ (wt%) | $Al_2O_3$ (wt%) | $FeO^{total}$ (wt%) |
|---|---|---|---|---|---|
| Basanite | Pre-run | 43.96 (0.46) | 2.71 (0.12) | 15.87 (0.23) | 9.92 (0.08) |
| Basanite | Post-run | 43.44 (0.51) | 2.68 (0.11) | 15.92 (0.21) | 10.01 (0.12) |
| Andesite | Pre-run | 52.24 (0.49) | 0.29 (0.05) | 15.33 (0.14) | 8.62 (0.11) |
| Andesite | Post-run | 51.99 (0.48) | 0.27 (0.07) | 15.45 (0.20) | 8.80 (0.13) |
| Dacite | Pre-run | 61.97 (0.51) | 0.67 (0.07) | 17.76 (0.18) | 4.55 (0.08) |
| Dacite | Post-run | 62.00 (0.43) | 0.62 (0.08) | 17.59 (0.14) | 4.72 (0.15) |
| Pantellerite | Pre-run | 67.28 (0.43) | 0.50 (0.05) | 11.96 (0.12) | 5.59 (0.12) |
| Pantellerite | Post-run | 66.94 (0.56) | 0.54 (0.07) | 11.39 (0.14) | 6.07 (0.15) |

| Sample | MgO (wt%) | CaO (wt%) | $Na_2O$ (wt%) | $K_2O$ (wt%) | Total |
|---|---|---|---|---|---|
| Basanite | 9.56 (0.11) | 12.14 (0.11) | 3.03 (0.13) | 1.45 (0.10) | 98.64 |
| Basanite | 9.66 (0.19) | 12.48 (0.18) | 2.97 (0.17) | 1.21 (0.10) | 98.37 |
| Andesite | 7.62 (0.10) | 11.32 (0.10) | 2.34 (0.14) | 0.61 (0.08) | 98.37 |
| Andesite | 7.51 (0.16) | 10.91 (0.12) | 2.32 (0.15) | 0.70 (0.05) | 97.95 |
| Dacite | 2.33 (0.18) | 5.39 (0.18) | 4.77 (0.17) | 1.25 (0.06) | 98.68 |
| Dacite | 2.41 (0.13) | 5.71 (0.11) | 4.82 (0.16) | 1.13 (0.09) | 99.00 |
| Pantellerite | 0.13 (0.14) | 0.50 (0.17) | 6.88 (0.18) | 5.18 (0.06) | 98.02 |
| Pantellerite | 0.19 (0.18) | 0.61 (0.11) | 6.94 (0.17) | 5.43 (0.11) | 98.11 |

Standard deviations indicated in parentheses

tion of tetrahedral over octahedral $Fe^{3+}$ with increasing basicity ($CaO:SiO_2$ ratio) of the calcium-iron-silica (CFS) glasses. The two compositions chosen for calorimetric measurements (no. A and no. B; Kress and Carmichael 1989) have very different $X_{CaO}$: $X_{SiO_2}$ ratios, suggesting different populations of $Fe^{3+}$ in octahedral and tetrahedral coordination. From the volume data (Lange and Carmichael 1990: Fig. 1), composition CFS-B is anticipated to contain $Fe^{3+}$ primarily in tetrahedral coordination, whereas composition CFS-A may contain $Fe^{3+}$ in both 4- and 6-fold coordination. If this *assumption* is correct, it may explain the higher measured heat capacities of the CFS-A melt relative to those predicted by the model as more than one coordination for $Fe^{3+}$ may increase the configurational contribution to the liquid heat capacity. In other words, the presence of *more than one* coordination state for $Fe^{3+}$, with an absorption of heat as the proportions change with changing temperature, may increase the liquid $Cp$ value. Unfortunately, the experimental temperature range accessible for this sample is not sufficient to examine any unusual temperature dependence to its liquid heat capacity.

### *Application to natural liquids*

The measured heat capacities of the four natural samples were used to evaluate whether the heat capacity model presented in this study (calibrated primarily on simple 3- and 4-component silicate melts) can be applied to

multicomponent, magmatic compositions. In order to assess the applicability of the model to igneous liquids, the heat capacity measurements on the four natural melts were removed from the data base and partial molar heat capacity values for the oxide components were re-derived using Eq. 8. These values were used to calculate the heat capacities of the natural melts; they deviate from the measured values within 1.9% on average, with the largest discrepancy off by 4.0%. For comparison, the models of Stebbins et al. (1984) and Richet and Bottinga (1985) reproduce the measured heat capacites of the natural liquids within 2.5 and 2.2% respectively and the sodic and calcic iron-bearing liquids (excluding CFS-A) within 3.1 and 4.3% respectively. We conclude, therefore, that our model (assuming no excess heat capacity) can predict the heat capacities of anhydrous igneous melts well within the experimental and interlaboratory errors. Perhaps more importantly, this study demonstrates that step-scanning calorimetry can be used to measure the heat capacities of natural melts where knowledge of *both* the ferric-ferrous ratio *and* the oxygen fugacity of the sample are required. This is particularly important in applications where the enthalpy of a crystallizing magma is measured "in-situ" along a specified $fO_2 - T$ path.

**Appendix 2.** Data from the literature used to calibrate the $Cp$ model of this study

| Sample | $Cp \pm 1\sigma$[a] (J/g.f.w.-K) | Reference |
|---|---|---|
| $An_4Qtz$ | 93.99 ± 1.96 | Stebbins et al. (1984) |
| $An_{35}Di_{65}$ | 92.41 ± 1.12 | Stebbins et al. (1984) |
| $Ab_{40}An_{35}Di_{25}$ | 100.82 ± 2.49 | Stebbins et al. (1984) |
| $Ab_{40}An_{20}Di_{40}$ | 95.46 ± 1.08 | Stebbins et al. (1984) |
| $Ab_{15}An_{10}Di_{75}$ | 86.15 ± 2.28 | Stebbins et al. (1984) |
| $Ab_{20}An_{60}Di_{20}$ | 96.23 ± 5.33 | Stebbins et al. (1984) |
| $Ab_{75}Di_{25}$ | 90.30 ± 1.38 | Stebbins et al. (1984) |
| $Ab_{50}Di_{50}$ | 95.51 ± 1.33 | Stebbins et al. (1984) |
| $An_{50}Di_{50}$ | 94.11 ± 3.02 | Stebbins et al. (1984) |
| $Ab_{25}Di_{75}$ | 96.04 ± 1.35 | Stebbins et al. (1984) |
| $Ab_{75}An_{25}$ | 98.86 ± 1.74 | Stebbins et al. (1982) |
| $Ab_{50}An_{50}$ | 105.76 ± 1.29 | Stebbins et al. (1982) |
| $Ab_{25}An_{75}$ | 111.35 ± 2.09 | Stebbins et al. (1982) |
| Sanidine | 93.61 ± 0.71 | Stebbins et al. (1983) |
| Nepheline | 110.68 ± 3.87 | Stebbins et al. (1983) |
| Albite | 92.96 ± 0.77 | Stebbins et al. (1983) |
| Diopside | 88.28 ± 1.08 | Stebbins et al. (1983) |
| No. 9 | 88.42 ± 0.47 | Carmichael et al. (1977) |
| Sphene | 93.16 ± 0.60 | King et al. (1954) |
| CMTS | 91.28 ± 2.31 | Lange and Navrotsky (1990) |
| $Na_2SiO_3$ | 88.58 ± 0.75 | Naylor (1945) |
| $Na_2Si_2O_5$ | 86.97 ± 0.39 | Naylor (1945) |
| Fayalite | 81.24 ± 3.06 | Stebbins and Carmichael (1984) |
| Anorthite | 107.95 ± 0.10 | Richet and Bottinga (1984a) |
| Andesine | 99.64 ± 0.21 | Richet and Bottinga (1984a) |
| Wollastonite | 83.71 ± 0.61 | Richet and Bottinga (1984a) |
| Diopside | 83.50 ± 0.08 | Richet and Bottinga (1984a) |
| Cordierite | 105.11 ± 0.12 | Richet and Bottinga (1984a) |
| Pyrope | 97.46 ± 0.05 | Richet and Bottinga (1984a) |
| Albite | 90.41 ± 0.34 | Richet and Bottinga (1984b) |
| Jadeite | 96.19 ± 0.37 | Richet and Bottinga (1984b) |
| Sanidine | 88.93 ± 0.63 | Richet and Bottinga (1984b) |
| Nepheline | 104.84 ± 0.33 | Richet et al. (1984b, 1990) |
| KS5 | 83.15 ± 0.17 | Richet and Bottinga (1985) |
| KS2 | 89.34 ± 0.29 | Richet and Bottinga (1985) |
| KS1.3 | 92.92 ± 0.49 | Richet and Bottinga (1985) |
| NS | 91.03 ± 0.34 | Richet et al. (1984) |
| NS2 | 88.56 ± 0.12 | Richet et al. (1984) |
| NS3 | 85.99 ± 0.08 | Richet et al. (1984) |
| NS6 | 84.15 ± 0.31 | Richet et al. (1984) |
| KS4 | 82.08 ± 0.52 | Richet and Bottinga (1980) |

[a] $Cp$ values were derived by fitting the reported enthalpy measurements to the following regression equation: $H_T - H_{298} = a + bT$, where $b = Cp$. The standard error ($1\sigma$) is the fitted error on the coefficient $b$

*Acknowledgements.* This work was supported by the National Science Foundation (Grant EAR 8803215). Ian Carmichael generously provided the samples for this study. We are grateful to Jonathan Stebbins and Don Dingwell for constructive reviews.

## References

Apps JA, Niel JM (1978) Selected albites as candidates for hydrothermal solubility measurements, In: Fundamental geoscience program report, 1977, LBL-7058. Lawrence Berkeley Lab, Berkeley, pp 10–13

Bowker JC, Lupis CHP, Flinn PA (1981) Structural studies of slags by Mössbauer spectroscopy. Can Metall Q 20:69–78

Carmichael ISE, Nicholls J, Spera FJ, Wood BJ, Nelson SA (1977) High temperature properties of silicate liquids: applications to the equilibrium and ascent of basic magma. Philos Trans R Soc London A286:373–431

Delaney PT (1988) Fortran 77 programs for conductive cooling of dikes with temperature-dependent thermal properties and heat of crystallization. Comput Geosci 14:181–212

Dingwell DB, Brearley M (1988) Melt densities in the $CaO-FeO-Fe_2O_3-SiO_2$ system and the compositional dependence of the partial molar volume of ferric iron in silicate melts. Geochim Cosmochim Acta 52:2815–2825

Dingwell DB, Brearley M, Dickinson JE (1988) Melt densities in the $Na_2O-FeO-Fe_2O_3-SiO_2$ system and the partial molar volume of tetrahedrally coordinated ferric iron in silicate melts. Geochim Cosmochim Acta 52:2467–2475

Ghiorso M, Carmichael ISE (1985) Chemical mass transfer in magmatic process, II: applications in equilibrium crystallization, fractionation and assimilation. Contrib Mineral Petrol 90:121–141

Ghiorso M, Carmichael ISE, Rivers ML, Sack RO (1983) The Gibbs free energy of mixing of natural silicate liquids; an expanded regular solution approximation for the calculation of magmatic intensive variables. Contrib Mineral Petrol 84:107–145

Iwamoto N, Tsunawaki Y, Nakagawa H, Yoshimura T, Wakabayashi N (1978) Investigations of calcium-iron-silicate glasses by the Mössbauer method. J Non-Cryst Solids 29:347–356

Jaeger JC (1968) Cooling and solidification of igneous rocks. In: Hess HH, Poldevardt A (eds) Basalts (Poldervaardt treatise on rocks of basaltic composition, vol. 2) John Wiley and Sons, New York, pp 503–536

Johnson T (1990) The partial molar volume of $TiO_2$ in multicomponent silicate melts. M.S. Thesis, University of California, Berkeley

King EG, Orr RL, Bonnickson KR (1954) Low-temperature heat capacity, entropy at 298.16 K and high-temperature heat content of sphene ($CaTiSiO_5$). J Am Chem Soc 70:4320–4321

Kress VC, Carmichael ISE (1988) Stoichiometry of the iron oxidation reaction in silicate melts. Am Mineral 73:1267–1274

Kress VC, Carmichael ISE (1989) The lime-iron-silica melt system: redox and volume systematics. Geochim Cosmochim Acta 53:2883–2892

Lange RA, Carmichael ISE (1987) Densities of $Na_2O-K_2O-CaO-MgO-FeO-Fe_2O_3-Al_2O_3-TiO_2-SiO_2$ liquids: new measurements and derived partial molar properties. Geochim Cosmochim Acta 51:2931–2946

Lange RA, Carmichael ISE (1989) Ferric-ferrous equilibria in $Na_2O-FeO-Fe_2O_3-SiO_2$ melts: effects of analytical techniques on derived partial molar properties. Geochim Cosmochim Acta 53:2195–2204

Lange RA, Carmichael ISE (1990) Thermodynamic properties of silicate liquids with an emphasis on density, thermal expansion and compressibility. In: J Nicholls, JK Russell (eds) Modern Methods of Igneous Petrology: Understanding Magmatic Processes. (Reviews in Mineralogy 24) Mineral Soc Am, Washington, D.C., pp 25–64

Lange RA, Navrotsky A (1990) Heat capacities of $TiO_2$-bearing silicate liquids. Trans Am Geophys Union 71:1650

Lange RA, De Yoreo JJ, Navrotsky A (1991) Scanning calorimetric measurement of heat capacity during incongruent melting of diopside. Am Mineral 76:904–912

Morinaga K, Suginohara Y, Yanagase T (1976) J Jpn Inst Metals 40:480–489

Navrotsky A, Ziegler D, Oestrike R, Manier P (1989) Calorimetry of silicate melts at 1773 K: measurement of enthalpies of fusion and of mixing in the systems diopside-anorthite-albite and anorthite-forsterite. Contrib Mineral Petrol 101:122–130

Naylor BF (1945) High temperature heat contents of sodium metasilicate and sodium disilicate. J Am Chem Soc 67:466–467

Nekvasil H (1988) Calculation of equilibrium crystallization paths of compositionally simple hydrous felsic melts. Am Mineral 73:956–965

Pargamin L, Lupis CHP, Flinn PA (1972) Mössbauer analysis of the distribution of iron cations in silicate slags. Metall Trans 3:2093–2105

Richet P, Bottinga Y (1980) Heat capacity of liquid silicates: new measurements on $NaAlSi_3O_8$ and $K_2Si_4O_9$. Geochim Cosmochim Acta 44:1535–1541

Richet P, Bottinga Y (1984a) Anorthite, andesine, wollastonite, diopside, cordierite and pyrope: thermodynamics of melting, glass transitions, and properties of the amorphous phases. Earth Planet Sci Lett 67:415–432

Richet P, Bottinga Y (1984b) Glass transitions and thermodynamic properties of amorphous $SiO_2$, $NaAlSi_nO_{2n+2}$ and $KAlSi_3O_8$. Geochim Cosmochim Acta 48:453–470

Richet P, Bottinga Y (1985) Heat capacity of aluminum-free liquid silicates. Geochim Cosmochim Acta 49:471–486

Richet P, Bottinga Y, Tequi C (1984) Heat capacities of sodium silicate liquids. J Am Ceram Soc 67:C6–C8

Richet P, Robie RA, Rogez J, Hemingway BS, Courtial P, Tequi C (1990) Thermodynamics of open networks: ordering and entropy in $NaAlSiO_4$ glass, liquid, and polymorphs. Phys Chem Miner 17:385–394

Robie RA, Hemingway BS, Fisher JR (1978) Thermodynamic properties of minerals and related substances at 298.15 K and 1 bar ($10^5$ pascals) pressure and at high temperatures. US Geol Surv Bull 1452

Stebbins JF, Carmichael ISE (1984) The heat of fusion of fayalite. Am Mineral 69:292–297

Stebbins JF, Weill DE, Carmichael ISE, Moret LK (1982) High temperature heat contents and heat capacities of liquids and glasses in the system $NaAlSi_3O_8-CaAl_2Si_2O_8$. Contrib Mineral Petrol 80:276–284

Stebbins JF, Carmichael ISE, Weill DE (1983) The high temperature liquid and glass heat contents and the heats of fusion of diopside, albite, sanidine and nepheline. Am Mineral 68:717–730

Stebbins JF, Carmichael ISE, Moret LK (1984) Heat capacities and entropies of silicate liquids and glasses. Contrib Mineral Petrol 86:131–148

Weill DF, Hon R, Navrotsky A (1980) The igneous system $CaMgSi_2O_6-CaAl_2Si_2O_8-NaAlSi_3O_8$: variations on a classic theme by Bowen. In: RB Hargraves (ed) Physics of Magmatic Processes. Princeton University Press, pp 49–92

Editorial responsibility: T. Grove